INVITED PAPER

A Review of Phased Array Steering for Narrow-Band Electrooptical Systems

Rapid, accurate, non-mechanical techniques for steering optical beams can provide the kind of efficient random access pointing offered by microwave radars.

By Paul F. McManamon, *Fellow IEEE*, Philip J. Bos, Michael J. Escuti, *Member IEEE*, Jason Heikenfeld, *Senior Member IEEE*, Steve Serati, Huikai Xie, *Senior Member IEEE*, and Edward A. Watson

ABSTRACT | Nonmechanical steering of optical beams will enable revolutionary systems with random access pointing, similar to microwave radar phased arrays. An early approach was birefringent liquid crystals writing a sawtooth phase profile in one polarization, using 2π resets. Liquid crystals were used because of high birefringence. Fringing fields associated with voltage control required to implement the 2π resets have limited the efficiency and steering angle of this beam steering approach. Because of steering angle limitations, this conventional liquid crystal steering approach is usually combined with a large angle step-steering approach. Volume holograms, birefringent prisms or sawtooth-profile birefringent phase gratings, and circular-type polarization gratings are the large angle step steering approaches that will be reviewed in this paper. Alternate steering approaches to the combined liquid crystal and step-steering approach exist. Microelectromechanical system mirrors, lenslet arrays, electrowetting, and a variable birefringent grating approach will be reviewed and compared against the conventional liquid crystal and step-steering approaches. Step-steering approaches can also be combined with these approaches. Multiple nonmechanical steering approaches are developing that will allow high-efficiency steering, excellent steering accuracy, and wide fields of view.

KEYWORDS | Beam steering; nonmechanical beam steering; optical phased arrays; spatial light modulators

I. INTRODUCTION

Steering and stabilizing are still major limitations of electro-optical systems such as laser radar. Mechanical pointing and stabilization are still the norm, limiting rapid pointing ability, maintaining a high mechanical complexity, keeping reliability low, and keeping costs high. Nonmechanical approaches to increase pointing speed, provide random access pointing, decrease complexity, increase reliability, and reduce costs can make a major impact on future optical systems.

The challenge for nonmechanical beam steering is that, for many applications, we desire both to steer to a large angle ($+/-45^\circ$ or more) and to have reasonably large apertures (5 cm or more). This implies a very large number of steering states (defined in one dimension as the total steering angle divided by the diffraction-limited angular spot size). Related to the number of steering states is the Lagrange invariant. This invariant is a property of the optical system and does not change with propagation through the system, including components like telescopes. At a pupil plane (in air), the Lagrange invariant is defined as the product of the radius of the pupil times the tangent of the maximum steering half-angle. Hence, for the specifications above, we are interested

Manuscript received December 2, 2008; revised January 30, 2009.
Current version published May 13, 2009
P. F. McManamon is with Exciting Technology LLC, Dayton, OH 45424 USA (e-mail: paul@excitingtechnology.com).
P. J. Bos is with the Liquid Crystal Institute, Kent State University, Kent, OH 44242 USA (e-mail: pbos@kent.edu).
M. J. Escuti is with the North Carolina State University at Raleigh, Raleigh, NC 27606 USA (e-mail: mjescuti@ncsu.edu).
J. Heikenfeld is with the University of Cincinnati, Cincinnati, OH 45221 USA (e-mail: heikenjc@email.uc.edu).
S. Serati is with the Boulder Nonlinear Systems, Inc., Lafayette, CO 80026 USA (e-mail: sserati@bnonlinear.com).
H. Xie is with the University of Florida, Gainesville, FL 32611 USA (e-mail: hkx@ufl.edu).
E. A. Watson is with the Air Force Research Laboratory, Wright-Patterson AFB, OH 45433 USA (e-mail: Edward.Watson@WPAFB.AF.MIL).

Digital Object Identifier: 10.1109/JPROC.2009.2017218

in Lagrange invariants on the order of 2.5 cm or larger. To achieve this value, we have typically found the need to implement nonmechanical steering with at least two stages: a large-angle discrete steering stage and a small-angle continuous steering stage [1].

A large number of nonmechanical beam steering technologies have been investigated. We review some of those in this paper. The remainder of this paper is organized as follows. We begin by describing the basic physics of nonmechanical beam steering, which leads to a means to categorize the beam-steering approaches. We then discuss several steering technologies that have been developed and indicate for which category they are most suitable. Some of the more promising technologies will be described in more detail in later sections.

A. Physics of Nonmechanical Beam Steering

We can understand the physics of nonmechanical beam steering by considering the effect of a prism on an incident beam normal to a surface. The index of refraction in a prism is larger than that of air, so light travels more slowly within the prism. The angle of light passing through a prism will be changed because the light moving through the thick portion of the prism will be delayed compared to light traveling through the thin portion. Steering can be accomplished by changing the thickness of the prism.

Light could be steered electronically by writing a prism. The problem is that it is difficult to create an optical path difference (OPD) as large as would be required to write a full prism of appreciable width. For example, a 10-cm-wide aperture steering to 30° would require >5 cm OPD on the thick side of the prism.

For a narrow wavelength, we can take advantage of the fact that light is a sine wave. With sine waves it does not matter if we have 0, 2π, 4π, or $2n\pi$ phase shift. From a phase point of view, they are all the same. Therefore, as one moves across the width of the prism, one can subtract 2π of phase every time the phase reaches 2π, resulting in a sawtooth phase profile. The unfolded phase, which is called a modulo 2π phase profile, looks like the phase profile that would result from propagation through a full prism, and steers light in the same manner. This is shown in Fig. 1. The benefit of using a modulo 2π phase profile is

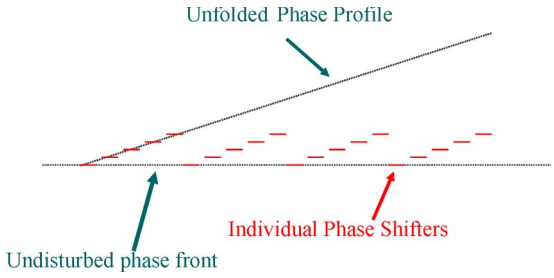

Fig. 1. *Modulo 2π phase shifting to create beam steering.*

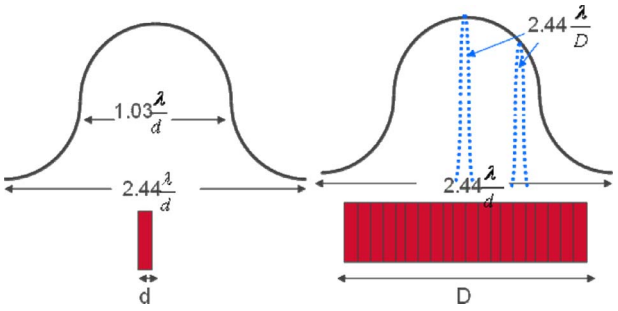

Fig. 2. *The envelope under which beam steering occurs.*

that the required OPD can be small. The maximum required OPD is approximately equal to the wavelength of the light being used. The modulo 2π steering approach does make the beam steerer very wavelength-dependent (dispersive) [2], [3].

The largest angle one can steer to using the modulo 2π approach is determined by the size of the smallest individually addressable phase element. If you illuminate the full array of phase shifters with a Gaussian beam, then any individual phase shifter will have an approximately uniform irradiance distribution across it. For a circular aperture uniformly illuminated, the full width beam divergence at the half power point is [4]:

$$\theta \cong \frac{1.03 * \lambda}{d} \tag{1}$$

where $\theta =$ beam divergence, $\lambda =$ wavelength of the electromagnetic radiation, and $d =$ the width of the individual radiator. If phase can be locked among many individual radiators, the beam will become narrower in angle proportional to the increase in the effective size of the radiator. If the full array is uniformly illuminated, then we can substitute

$$D = nd \tag{2}$$

into (1), where n is the number of individual radiators assembled to make the large radiator and where we have assumed that the pitch of the radiator separations is equal to the width of the radiator (i.e., unity fill factor). For Gaussian illumination of the full array, the effective size of the large aperture is reduced and the beam divergence increases. The allowed amount of clipping of the Gaussian beam by the aperture array determines how much the effective aperture size is reduced. By adjusting the phasing among the individual elements, the narrow beam can be steered under the envelope of the larger beam resulting from an individual radiator. Fig. 2 shows this for uniform illumination.

Phased array microwave radars steer to angles larger than 45°. To do this, the radars use individual radiators that are at a half-wavelength spacing or closer. In radar, the conventional discussion of half-wavelength spacing says individual phase adjustable radiators must be no larger than half-wavelength to reduce grating lobes [5]. This is a different view of the same physics. From (1), if d equals one-half of λ, then $\theta = 2.06$ rad or 118°. This is the full beam width at the half power points. We could steer plus or minus 45° and still be above the half power point, neglecting the cosine factor loss in the projected area of the aperture.

The modulo 2π phase shift approach shown in Fig. 1 is essentially a blazed transmission grating. The periodic sawtooth phase profile results in efficient deflection of the light into one diffraction order of the grating if the blaze is constructed properly. In nonmechanical beam steering, the parameters of the grating are electronically controlled, making them dynamic gratings. Consider the grating equation

$$\sin\theta = \frac{m\lambda}{A} \tag{3}$$

where θ is the steering angle, m is the order of steering associated with the grating, λ is the wavelength of light, and A is the period of the grating. There are two basic approaches to beam steering using sawtooth dynamic gratings [6]. One approach is to vary the period A. This is done by controlling the number of phase shifters that are contained within one period of the grating. Variable period beam steering is shown in Fig. 3. In this approach, the grating is blazed to steer to the first order $(m = 1)$. The OPD monotonically increases until it equals one wavelength of a design wavelength. Then we subtract one wavelength, or 2π phase, from the OPD. For variable period beam steering, the period before a one-wavelength reset is smaller when we steer to larger angles. The largest angle we can steer to efficiently is determined by the smallest allowed period between resets.

Another approach to beam steering using sawtooth dynamic gratings is to vary the blaze of the grating, which varies the order m to which energy is efficiently steered. This is implemented by allowing the maximum OPD to take on values up to many wavelengths. The period between resets is constant but the varying blaze results in energy's being steered to different angles, or orders. Variable blaze beam steering is shown in Fig. 4. It can be seen that variable blaze beam steering only steers to discrete angles where the value of the reset is a multiple of the wavelength, a multiple of 2π phase.

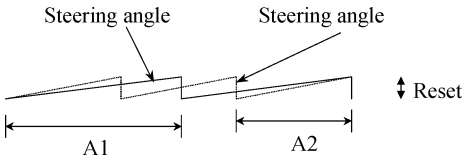

Fig. 3. *Variable period beam steering.*

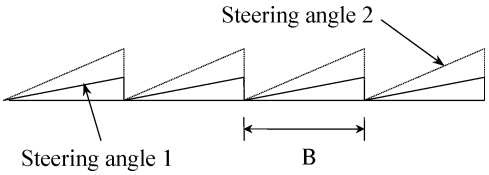

Fig. 4. *Illustration of variable blaze beam steering.*

In order to steer continuously in variable blaze beam steering, one can add a second, variable period dynamic grating. This can be implemented by placing a 0 to 2π phase layer underneath each fixed period of the variable blaze grating. By adjusting the phase on these layers under each fixed period, it is possible to move the location of the discrete steering angles [7].

B. Approaches to Nonmechanical Beam Steering

Early approaches to nonmechanical steering were undertaken by a number of workers. Beam steering based on the electro-optic effect was investigated in different materials, including lithium tantalate [8] as well as lithium niobate [9]. Typically these approaches did not lead to the large Lagrange invariant that we desire. Arrays of waveguides have also been investigated, e.g., in AlGaAs [10], but again waveguide arrays have a limited Lagrange invariant.

Liquid crystal technologies are of particular interest to us because of the potential to achieve the large Lagrange invariants we desire but at the same time can potentially be fabricated using well-established techniques, for example, liquid crystal displays [11]. Liquid crystals approaches have been investigated for a considerable number of years [12]. Liquid crystals have high birefringence, so can steer by creating a large OPD for one polarization using relatively modest voltages. Liquid crystal devices have been fabricated to implement both variable blaze [13] and variable period [14]–[16] steering. The variable period approach used an array of piston phase shifters to approximate a sawtooth phase profile with 2π phase resets under electronic control. Steering time is typically on the order of milliseconds.

While liquid crystal devices have several advantages, one important disadvantage has proven to be their steering efficiency at large angles. The issues with steering efficiency will be discussed in Section II, but a result of the low efficiency is that alternate techniques have been investigated for steering to large angles. The final steering system then often consists of a liquid crystal optical phased array for continuous steering over small angles combined with an alternate technique that provides steering to a discrete number of larger angles. The combination results in a system with continuous steering over large angular range.

A few different techniques for large angle discrete steering have been investigated. These are discussed in

detail in Section III, but we briefly mention them here. One technique is based on multiplexed volume holography. A limited number of gratings that steer to large angles are written into a holographic recording medium. A particular grating is addressed by small angle steering in front of the hologram. A second small angle steering device is used behind the hologram to provide continuous angle steering between the angles produced by the holograms [17], [18]. A second approach is birefringent prisms. In this case, a series of prisms are used that steer to one of two states depending on the polarization of the incident light. Only one continuous steering stage is required. Electronically controlled waveplates are used to alter the polarization before each prism to choose the binary direction of steering. The main difficulty of this approach is the thickness of prisms for large angles, resulting in the beam either being clipped by later stages of the beam steerer or requiring the aperture diameters to increase. A thinner alternative is fixed, modulo 2π, sawtooth-profile birefringent phase gratings. These gratings can provide wide angle step-steering stages [19]. The last wide-angle step-steering approach to be considered here can be described as circularly polarized liquid crystal birefringent polarization gratings, formed in bulk, surface aligned, liquid crystals. In the literature, these are referred to as liquid crystal polarization gratings (LCPGs) [20]. LCPGs have been demonstrated to have a diffractive efficiency exceeding 99.5%. These are a new class of liquid crystal gratings that generate phase shift using polarization rotation rather than varying the OPD. LCPGs have the same benefits from being thin as the OPD-based sawtooth gratings but have a linear, rather than sawtooth, phase profile [20]. Therefore, the discontinuity and thus the higher order diffraction due to imperfect modulo 2π resets and any shadowing due to those resets are eliminated. This difference will be further discussed in the paper.

While liquid crystal based optical phased array concepts and their associated large-angle steering techniques have received considerable attention over the years, a number of other approaches to developing phased arrays have been, and are being, investigated. One well-known approach is based on microelectromechanical systems (MEMS) [21]–[25]. The optical MEMS devices can be manufactured to implement a variable period approach to beam steering by fabricating a series of mirrors that move perpendicular to the substrate, imparting a piston phase to light reflected off the surface. Two issues with this approach are the minimum size of MEMS mirrors and the fill factor [26]. As discussed earlier, to have an ideal beam steerer using piston phase changes, we would like half-wavelength spacing or less between phase elements. This is impractical given current MEMS fabrication technology. Alternately, optical MEMS can be fabricated to implement a variable blaze approach. In this case, each mirror is tilted to produce the appropriate blaze to steer to the desired angle (see Fig. 5). Using a tilted sawtooth

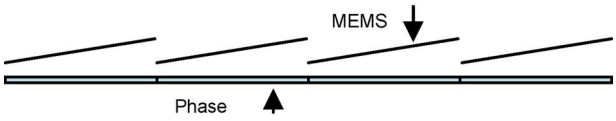

Fig. 5. ***Additional phase layer with MEMS mirrors.***

approach, the phase profile is perfect (assuming the micromirrors are flat) until the reset. The reset then must be 2π, $4\pi, \ldots,$ $2n\pi$ in phase, or an integral number of wavelengths, in order to have no phase discontinuity at the reset. This puts a strict requirement on the MEMS device to control the tilt of the micromirrors. We contrast this type of optical MEMS with the more standard amplitude modulation MEMS, in which the mirrors are used just to deflect light out of the optical path.

Since the MEMS approach is a variable blaze approach, an additional phase shift layer is required to produce continuous steering. An interesting alternative is to incorporate actuators with each mirror that also produce piston motion of the tilted mirrors. This concept is discussed more fully in Section IV.

The other restriction with MEMS mirrors is they need to be used in a reflective mode. This is a disadvantage since more compact systems can be built using transmissive optics, but for some applications this engineering restriction will be acceptable. Geometries exist that allow steering in both dimensions using reflective steering approaches.

Electrowetting can also be used as a method to steer optical beams [27]. This technique can generate a prism-like phase profile over a fixed period. These are variable blaze dynamic gratings. We require a zero to 2π phase layer to make the reset an integral number of wavelengths. If the phase layer can be adjusted, then this method can steer to a continuous set of angles. We need to make the space between prisms as small as possible to enhance fill factor. This approach is also discussed in Section IV.

We have looked at a set of three cascaded microlens arrays as another steering method [28]. This is also a variable blaze (fixed period) beam steerer, but it has no physical resets. There are virtual resets of the wavefront exiting the last microlens array. Only the first derivative of phase changes discontinuously in a physical layer. In theory, cascaded microlens array steering can obtain very high efficiency. The issue will be if we can obtain high efficiency in practice, due to the engineering complexity associated with making the microlenses uniform, high fill factor, and the need to have many layers. Microlens arrays are typically fabricated out of optical materials and are therefore static. However, we have also looked at generating microlens arrays in liquid crystal devices, in which case they can be dynamic, under electronic control. Lenslets can be solid, unchanging, devices or written. Static microlens arrays require micromotion to produce steering. Microlens arrays written into liquid crystal devices can be accurately controlled, and the

movement of the lenses can occur without any physical motion of the device.

Another approach to high-efficiency steering is called vertical-continuous optical phased arrays (V-COPA), a recent approach originated by Kent State [29]. This approach is based on the same underlying physics as the fixed LCPGs introduced earlier. In V-COPA, a continuous phase shift occurs without the need for a phase reset. As with the LCPGs, this approach directly generates a phase shift. There is no jump in either phase or any derivative of phase. In addition, the continuous phase shift is accomplished with a half-wavelength-thick layer of liquid crystal. This approach has shown very high deflection efficiency and is tunable in angle. This is an ideal beam-steering approach if various issues, such as speed of response, can be solved.

II. CLASSIC LIQUID CRYSTAL STEERING

By imposing an electric field, it is possible to change the index of refraction of a liquid crystal for light of a given polarization. We can write a sawtooth phase profile, discussed earlier, by using a series of small electrodes across from a ground plane, with a liquid crystal medium in between. Fig. 6 shows such a device.

The birefringence of the liquid crystal is produced by the rotation of the molecules under the applied voltage. Alignment layers create forces to make one orientation preferred in the absence of an electric field. An electric field can cause the molecules to reorient. Fig. 7 shows a liquid crystal cell in two different states: one with voltage applied and one without voltage applied.

Switching speed of a steering device is an important parameter. Speed of a liquid crystal steering device depends on how fast the liquid crystal molecules will rotate from one orientation to another. The relaxation time for a liquid crystal cell to return to its no-voltage state, once the electric field is removed, is given by

$$\tau_d = \frac{t^2 \gamma}{k\pi^2} \tag{4}$$

where

τ_d	time to return to no-voltage state;
t	cell thickness;
k	effective elastic constant;
γ	viscosity.

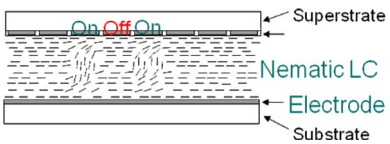

Fig. 6. ***A liquid crystal cell.***

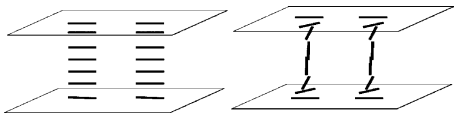

Fig. 7. ***Liquid crystal cell with voltage applied and without voltage applied.***

As can be seen from (4), cutting the cell thickness in half reduces switching time by a factor of four. Turnoff relaxation time is usually much slower than the time it takes to turn on the phase shift. Turn-on time is given by

$$\tau_r = \frac{\tau_d}{\left[\left(\frac{V}{V_t}\right)^2 - 1\right]} \tag{5}$$

where V = applied voltage and V_t = threshold voltage. We see that driving the turn-on with higher voltage speeds it up by approximately the square of the ratio of increased voltage.

Most liquid crystal based beam steerers to date have used nematic liquid crystals. For that case, the speeds are as described in (5) and (6). At high drive voltages, the turn-on time becomes much different than the turnoff time, so turnoff time is the majority of the speed limitation. To speed up the turnoff response, people have developed dual-frequency liquid crystals (DFLCs), which drive the molecules both on and off. This means (6) can be used for both turn on and turn off. With DFLCs, the dielectric properties of the material change sign as a function of the frequency of the applied ac voltage. As a result, the liquid crystal molecules are driven in different directions depending on the drive frequency, allowing the molecules to be driven into both states shown in Fig. 7. This complicates the electronic drivers since they must be able to drive the cell with two distinct frequencies, one above the critical frequency and one below [30], [31]. The critical frequency is nominally near 10 kHz for available DFLCs. Another possible method of speeding up liquid crystal beam-steering devices is by mixing polymers into the liquid crystals to effectively have many thinner cells [32]–[35]. A third method is to use smectic C liquid crystals instead of nematics [36].

Another important parameter for beam steering is steering efficiency, that is, how much of the light input to the steering unit is sent in the desired direction. There are two main efficiency considerations for liquid crystal beam steering. One is the flyback region, which is determined by fringing fields [37]. This effect is a result of the inability of the device to change its voltage profile instantaneously in space. The flyback region essentially reduces the fill factor of the grating. Equation (6) gives the efficiency due to flyback region effects. Fig. 8 shows that during the flyback

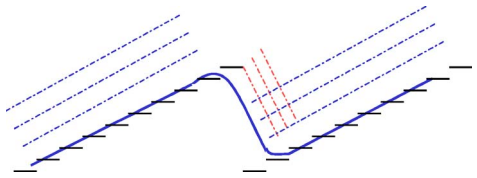

Fig. 8. *The effect of fringing fields on phase profile.*

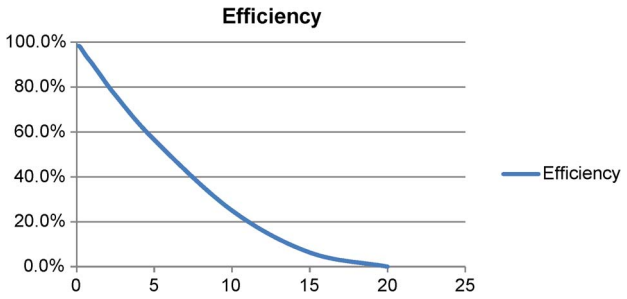

Fig. 9. *Efficiency versus angle limited by fringing field effects.*

portion of the phase profile, the beam is deflected in the wrong direction

$$\eta = \left(1 - \frac{\Lambda_F}{\Lambda}\right)^2. \tag{6}$$

Here η is efficiency, Λ_F is the width of the flyback region, and Λ is the width between resets [14].

Fig. 8 shows the fringing field difficulty for the liquid crystal approach. Fringing fields make it impossible to impose an electric field that stays only between the small electrodes. Instead, the field expands outward to each side of the small electrode. As a rule of thumb, the narrowest width of a voltage region above an electrode is about the thickness of the liquid crystal layer between the electrode and the ground plane [38]. Since the thickness of the liquid crystal layer is often larger than the spacing between the electrodes, it can be seen that fringing fields can have a significant effect. For transmissive beam steering, the cell has to be about as thick as required to obtain one wavelength, or 2π phase, of OPD. With a birefringence of 0.3, this means the cell has to be about 3.3 times one wavelength in thickness. For variable period beam steering, the steering angle in radians is approximately one wavelength divided by the distance between resets Λ. If we just use (6) as the loss in efficiency, then Table 1 gives efficiency for some interesting cases.

You can see from Table 1 and Fig. 9 that efficiency drops off very fast for conventional liquid crystal based beam steering. Unfortunately, if we want high efficiency, we need to limit the steering angles used for sawtooth phase profile liquid crystal continuous steering to very small angles. For a quarter of a degree angular steering, we only achieve about 98% steering efficiency. For 1° steering, we are down to 90% efficiency. If we need 1° steering in both azmuith and elevation, we need to square that loss. This is even a major limitation for use as the fine angle steering before a wide-angle course steering element. Imagine using holographic step steering as shown in Fig. 10 and having a 1° beam steerer before and after it, with steering in both azmuith and elevation. Just the fine-angle LC beam steerers result in almost 40% loss in efficiency.

Table 1 Efficiency Versus Angle Limited by Fringing Field Effects

Angle (deg)	Angle (rad)	Index change	Efficiency
20	0.349	0.35	0.0
15	0.262	0.35	6.3
10	0.175	0.35	25.0
5	0.087	0.35	56.5
2.5	0.044	0.35	76.4
1.5	0.026	0.35	85.7
1	0.017	0.35	90.5
0.625	0.011	0.35	93.8
0.25	0.004	0.35	97.7
0.15	0.003	0.35	98.3
0.1	0.002	0.35	98.9

The second contribution to steering efficiency is from the discrete nature of the phase steps. Equation (7) gives the loss in efficiency from using discrete steps

$$\eta = \left(\frac{\sin\left(\frac{\pi}{q}\right)}{\frac{\pi}{q}}\right)^2 \tag{7}$$

where η is efficiency and q is the number of steps in a ramp. Table 2 shows efficiency versus number of steps in a ramp.

Some early liquid crystal beam steering work avoided the loss associated with discrete steps, discussed above [13]. In this approach, a linear ramp in electric field was used instead of discrete phase steps. Initially it was not obvious which approach would be preferred, but the discrete steps did not provide a significant loss, and the

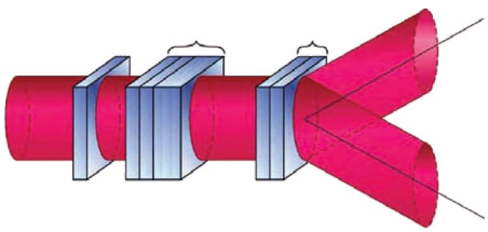

Fig. 10. *Holographic wide-angle steering.*

Table 2 Efficiency Versus Number of Steps in a Ramp

Efficiency vs. # of steps	
q	Efficiency
8	95.0%
10	96.8%
12	97.7%
16	98.7%
20	99.2%

linear region of the voltage versus phase shift was only a small portion of the full phase shift available from a liquid crystal cell, so it was necessary to make the LC cell thicker. The major loss using liquid crystal beam deflection had to do with fringing fields. This loss was not affected by using discrete steps versus a linear profile. The net result is the linear liquid crystal phase ramp approach to steering optical beams was not pursued further.

A third possible loss mechanism associated with liquid crystal beam steering devices is due to polarization [39], [40]. Especially near the phase resets, it is possible for polarization to be distorted, causing efficiency issues in later stages of steering.

III. LARGE-ANGLE DISCRETE STEERING

As mentioned earlier, optical phased arrays, and in particular liquid crystal optical phased arrays, require an alternate means to steer to large angles. Several of these are described in detail in this section.

A. Volume Holographic Step Steering

Volume (thick) holograms offer the potential to implement large-angle steering with high efficiency [41]. In this concept, a reference beam at a steering angle of interest is mixed with a signal beam in a holographic medium. Once the hologram is developed, it will diffract an incident signal beam into the direction of the reference beam, thereby steering the signal beam. Through the use of multiple holograms, multiple discrete steering angles can be addressed. These steering angles can be large, allowing us to achieve the large Lagrange invariants that we desire. A high fidelity, rugged medium for writing holograms is photothermal glass [42]. Holographic glass can be angle addressed or addressed with a more complex codes [17], [18], [43], [44]. For a variable wavelength source, these gratings can also be addressed by changing wavelength while keeping the angle constant [45]. The focus of this review paper is on steering approaches for narrow-band wavelength light, so angle addressing is the approach that will be reviewed here. With angle addressing, a beam steerer selects which hologram is addressed, resulting in the desired large angle of deflection. This scheme has the advantage of being able to use small angle continuous beam steering devices, such as the liquid crystal devices described in Section II, as the means to address the holograms without requiring technologies such as agile wavelength sources (which may not be permitted by the application) or unique phase encoding devices. Advances in volume holographic gratings in photothermal refractive glass make volume holograms a very interesting large-angle step-steering approach. Each glass holographic grating can have $>$ 99% efficiency [46], [47]. When two holograms are written in a single piece of glass, the efficiency can still be over 98% [48]. Losses due to scattering and absorption can be less than 0.5% for each holographic grating. These gratings are very capable of handling high power. As of now, the largest diameter holographic glass available is about 5 cm in diameter [46].

Many layers of holographic glass can be placed back to back with low loss. For example, we could use eight holograms in each direction, azimuth and elevation. If each hologram steers to an angle separated by five degrees from the adjacent angle, then we have a total field of regard of 40°, broken up into eight zones of 5° each. The incoming light is only diffracted by the holographic grating that has light input at the proper angle, and wavelength. There is no additional diffractive loss by using more gratings. More volume holograms do however introduce reflection, scattering, and absorption losses. In addition, the thickness of the grating stack increases. Only one grating in each dimension is set to steer light input at a given angle, dividing the steering into zones. Steering inside of each zone is referred to as filling each zone. This requires the use of a second beam steerer in each dimension after the stack of volume holograms. This wide-angle steering approach therefore requires two moderate angle, continuous, beam-steering devices, one before (for zone selection) and one after (for zone fill) the stack of volume holograms. Significant loses occur due to the low efficiency of traditional sawtooth-based liquid crystal small-angle continuous beam steerers before and after the holographic stack of gratings.

This steering approach has demonstrated continuous beam steering over a field of regard greater than 45° [37], [49]. The Raytheon patent on this technique claims the ability to steer at more than plus or minus 45° [18]. It would be possible to use this technique to steer both polarizations of light, but it would mean doubling the number of beam-steering elements.

If we want an 80° field of regard and 5° per step, then we would need to have 16 gratings in each dimension. Even at 0.5% loss per grating, that would mean a 16% loss when both dimensions are included. It will be critical to reduce losses per stage to a minimum if large-angle deflection is desired at high efficiency. A single piece of holographic glass is about 2 mm thick. This can cause limited walkoff issues in a large stack, due to 4 cm thickness for 20 gratings. By walkoff we mean the beam can move off the active area of the substrate or can hit the side wall because it is essentially steered inside of a tunnel.

B. Birefringent Prisms and Sawtooth Gratings

A second approach to wide-angle beam steering is to use birefringent prisms [50]–[54]. This technique also starts with a continuous beam steerer for small- to moderate-angle beam steering in each dimension. Larger angles are reached using a binary set of birefringent prisms. One polarization is deflected by the prism in one direction, while the other polarization is deflected in the other direction. Binary beam steering can be accomplished by rotating polarization between prism layers. A liquid crystal layer can be used to rotate polarization before each birefringent prism. Multiple prisms at factors of two in angular deflection allow for moderately large-angle beam steering. For example, if we once again take the case of a 40° field-of-regard continuous beam steerer, birefringent prisms would be needed for 2.5°, 5°, and 10°. Teledyne (formerly Rockwell Scientific) has pursued the birefringent prism approach for wide-angle steering. Teledyne has demonstrated steering out to plus or minus 20° using this approach. A difficulty with birefringent prism wide-angle beam steering is that the prisms get very thick at large angles. If a person were to use a birefringent material with a 0.2 birefringence, and had a 5-cm-diameter aperture, a 20° beam steerer would require a prism thickness of more than 8 cm. This thickness level causes significant problems with beam walkoff. If we had 20° steering at the beginning of an 8 cm tunnel, the walkoff would be almost 3 cm. This would require significant expansion of a 5-cm-diameter aperture to compensate for beam walkoff. A thick aperture must expand as the beam travels from the entrance of the aperture to the exit.

Currently, the largest birefringent prisms range from about 1 to 5 cm, depending on the material used. Prisms made from higher birefringence materials are available in smaller sizes. Some possible materials for birefringent prisms include calcite, which is a natural crystal. It is currently limited to 4–6 cm apertures. Another material is YVO4, a synthetic material, currently limited to 2–3 cm apertures, and Rutile, another synthetic. It has the highest birefringence and index but is currently limited to about 1 cm diameter.

Fig. 11 shows a stack of birefringent prisms, polarization rotators, and one continuous beam steerer to fill in between the digital angle steering available from the birefringent stack. One nice feature of birefringent prisms is that they can be designed for broad spectral band operation. They exhibit only material dispersion and not the diffractive dispersion associated with gratings. Another nice feature of this approach is that it only requires one small-angle continuous beam steerer for each dimension. The number of states you can steer to progresses geometrically, doubling with the addition of each new birefringent prism. For use with conventional sawtooth-based liquid crystal beam steerers, both of these features are very important to achieving high efficiency due to the rapid decrease in efficiency versus angle.

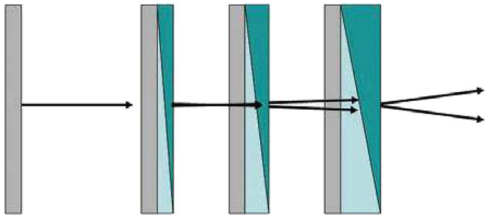

Fig. 11. ***Birefringent prism steering.***

A fundamentally similar, but much thinner, step-steering approach to wide-angle step steering is to use sawtooth profile phase gratings that act on a single linear polarization. Fig. 1 shows how, for a single wavelength, a modulo 2π sawtooth profile can be expended to act in phase like a prism. A fixed sawtooth phase profile can be written either by varying index of refraction in a medium of constant thickness or by varying thickness of a material. Sawtooth birefringent gratings can be switched in or out of the optical path by changing polarization, such as is done with the birefringent prisms discussed above, allowing thinner digital beam deflector architectures [19]. Alternately, switchable sawtooth phase gratings could also be used in the same manner. In the early 1990s, switchable liquid crystal holographic optical elements such as diffractive gratings and lenses were being developed [55]–[57]. Each sawtooth phase grating stage can double the maximum steered angle in one dimension, just like with switchable polarization prisms. Gratings are thin, so large steered angles are possible. Like the birefringent prisms, it only requires a single stage of fine angle steering before the wide-angle steering. This is in contrast to holographic wide-angle steering that requires fine-angle steering both before and after the holographic stack of glass. These gratings create a sawtooth profile in OPD, resulting in a sawtooth profile in phase, which can be unfolded exactly for a single wavelength. There should not be any fringing field loss, but there can be loss due to shadowing near the reset. In a large stack of gratings, these losses can accumulate. Potential efficiency per grating stage is the main issue with this approach for many digital stages of wide-angle step steering.

C. Liquid Crystal Polarization Grating

A fourth wide-angle step-steering approach is based on circular polarized gratings formed in bulk, surface aligned, liquid crystals. In the literature, these are called liquid crystal polarization gratings (LCPGs) [20]. Nonmechanical beam-steering approaches discussed until now rely on creating OPD, which is equivalent to a phase delay. There is an alternate approach that directly creates a phase delay. Fig. 12 shows the optical model of the quarter-waveplate, half-waveplate, quarter-waveplate (QHQ) device of Pancharatam [58]. A light beam passes through a polarizer,

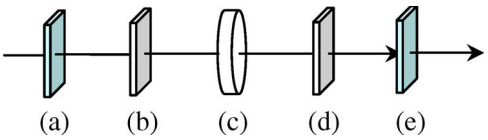

Fig. 12. *A basic setup of QHQ stack: (a) and (e) polarizer; (b) and (d) quarter-wave plate; and (c) half-wave plate.*

a quarter-wave plate ($\lambda/4$ plate), a half-wave plate ($\lambda/2$ plate), another quarter-wave plate, and another polarizer.

Linear incident light becomes circular polarized after the first $\lambda/4$ plate, which can be defined as E_{in} according to Jones calculus notation

$$E_{\text{in}} = \begin{bmatrix} Ex_{\text{in}} \\ Ey_{\text{in}} \end{bmatrix} = \begin{bmatrix} Ex_{\text{in}} \\ i \bullet Ex_{\text{in}} \end{bmatrix}. \tag{8}$$

For convenience, we assume it is a right-hand circular polarized light. E_{xin} and E_{yin} are vector components along the x and y-axis, respectively. The transmitted light E_{out} is defined as a linear mapping of the incident light E_{in} by a Jones matrix, which represents the $\lambda/2$ plate

$$E_{\text{out}} = \begin{bmatrix} \cos\beta & -\sin\beta \\ \sin\beta & \cos\beta \end{bmatrix} \bullet \begin{bmatrix} 1 & 0 \\ 0 & e^{i\varphi} \end{bmatrix} \bullet \begin{bmatrix} \cos\beta & \sin\beta \\ -\sin\beta & \cos\beta \end{bmatrix} \bullet \begin{bmatrix} Ex_{\text{in}} \\ i \bullet Ex_{\text{in}} \end{bmatrix} \tag{9}$$

where β represents the angle between the slow axis of the half-wave plate and the x-axis and φ is denoted as the phase retardation of the half-wave plate, which is equal to π. The final relationship can be simplified as

$$E_{\text{out}} = \begin{bmatrix} Ex_{\text{in}} e^{i \bullet 2\beta} \\ -i \bullet Ex_{\text{in}} e^{i \bullet 2\beta} \end{bmatrix}. \tag{10}$$

In the last expression, the transmitted light is a left-hand circular polarized light with a common phase factor $e^{i \cdot 2\beta}$, which is the most important result from the simple model. The phase of the transmitted circular light can be accurately controlled by the azimuth angle β. If β varies horizontally from 0 to π, the spatial phase profile of transmitted light will vary horizontally from 0 to 2π. If we have an LC cell with an in-plane director, the azimuth angle linearly rotating from 0 to π, and the total OPD across the cell agreeing with the half-wave retardation for the design wavelength, then the final spatial phase profile of transmitted light will linearly change from 0 to 2π. By duplicating this spatial director configuration repeatedly, an LC grating without any flyback or reset can be created. The amazing thing is that the cell is only one half-wave OPD thick. The flyback, or reset, is eliminated in this device. The thin cell gap reduces light scatting and adsorption of the liquid crystal cell. With this type of device, even though the optical thickness is only half-wave, it is possible to create a constant large phase gradient over an aperture size only limited by manufacturing constraints.

LCPGs with nearly ideal diffraction efficiencies ($> 99.5\%$) have been experimentally demonstrated over a wide range of grating periods, wavelengths (visible to near-infrared), and areas (many square centimeters) [59]–[62]. Each polarization grating stage can double the maximum steered angle in one dimension without major efficiency reductions, so very large steered angles are possible (at least to $\pm 40^\circ$ field of regard). Like the birefringent prisms and sawtooth phase gratings, it only requires a single stage of fine-angle steering before the wide-angle steering. This is in contrast to volume holographic wide-angle steering that requires fine-angle steering both before and after the holographic stack of glass. Fig. 13 shows ternary steering as compared to the binary steering shown in Fig. 11.

The structure at the heart of these devices is a polarization grating (PG), implemented using nematic liquid crystals (optionally switchable, or polymerizable), as shown in Fig. 14. The nematic director is a continuous in-plane bend-splay pattern established using an ultraviolet polarization hologram exposing photoalignment materials. When voltage is applied, the director orients out of plane, effectively erasing the grating. Diffraction occurs according to the following:

$$\eta_{m=0} = \cos^2\left(\frac{\pi \Delta n d}{\lambda}\right) \tag{11}$$

$$\eta_{m=\pm 1} = \left[\frac{1 \mp S_3'}{2}\right] \sin^2\left(\frac{\pi \Delta n d}{\lambda}\right) \tag{12}$$

where η_m is the diffraction efficiency of the mth-order, λ is the wavelength of incident light, and $S_3' = S_3/S_0$ is the normalized Stokes parameter corresponding to ellipticity of incident light. The grating equation (3) applies. Note that only these three orders are possible, and that when the

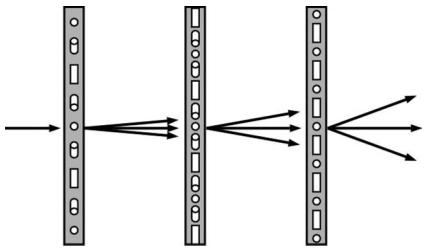

Fig. 13. *Ternary polarization grating steering.*

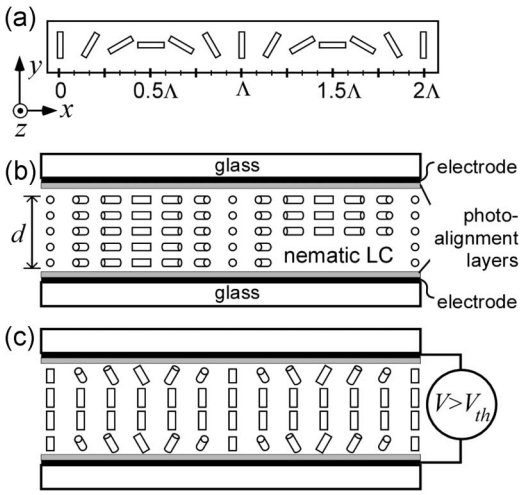

Fig. 14. *Director profile of liquid crystal polarization gratings. (a) shows the top view; (b) and (c) shown the side view in the zero and high voltage cases, respectively.*

retardation of the LC layer is half-wave ($\Delta nd = \lambda/2$), then 100% of the incident light can be directed out of the zeroth order. Note further that when the input polarization is circular, then all light can be directed into a single first order, with the handedness ($S_3' = \pm 1$) selecting the diffraction order (Fig. 13). Fig. 15 shows experimental validation of the extremely high steering efficiency.

A single LCPG can be considered the key component within digital beam steerer with three possible directions ($\pm\theta$ and 0°), as identified in Fig. 13. For the nondiffracting case, an applied voltage reduces the effective birefringence toward zero ($\Delta n \rightarrow 0$). LCPGs may also be fabricated with polymerizable liquid crystals, also known as reactive mesogens, and would therefore be fixed indefinitely. The practical advantages of these passive PGs (over the switchable, or active, PGs) are that they tend to manifest less scattering losses and allow for smaller grating periods.

While Crawford *et al.* originally conceived the circular LCPG in its switchable and polymer [63] forms, and demonstrated their basic diffraction behavior, their experimental results showed low efficiencies ($\leq$ 8%) and were limited to small diffraction angles. Subsequently, Escuti *et al.* developed materials and processing methods that produced defect-free, nearly ideal PGs with $>$ 99.5% experimental diffraction efficiency (in the switchable [64]–[66] and polymer [67] variants) and grating periods from ≥ 5 μm as a representative example [63]. Fig. 16 shows measured efficiency in each order, with an inset image of the LCPG as seen within a polarizing optical microscope. Low loss due to scatter has been demonstrated ($<$ 0.3%). A subsequent report by Cipparrone *et al.* [69] achieved similarly high-quality switchable gratings using different materials. More recent work by Escuti *et al.* has developed polymer PGs down to 1 μm. This proven ability to experimentally realize nearly ideal PGs at almost any aperture size is the key innovation that enables the wide-angle beam steering described in this section.

Two primary configurations of LCPGs and variable LC $\lambda/2$-waveplates are shown in Fig. 17 that can implement a single wide-angle beam steering stage. The passive approach has the primary advantage that the maximum steering angle is twice as large as the active approach, for identical grating periods. The active approach has the advantage that only one PG is required per stage, and therefore has potentially lower scattering losses. The comparative advantages of each approach are being studied [20].

Multiple stages may be cascaded to implement a coarse, binary beam steerer (Fig. 18). Furthermore, a

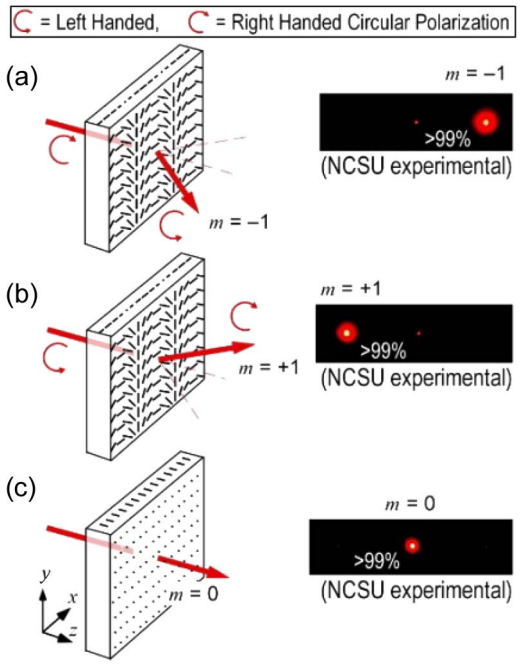

Fig. 15. *Beam steering with single LCPG.*

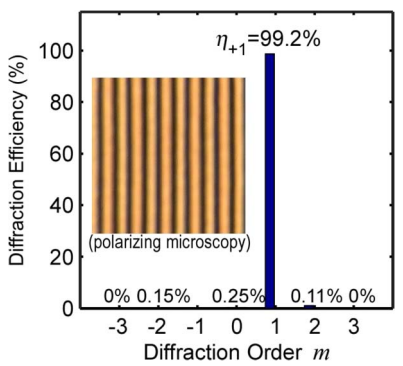

Fig. 16. *Measured diffraction from LCPG.*

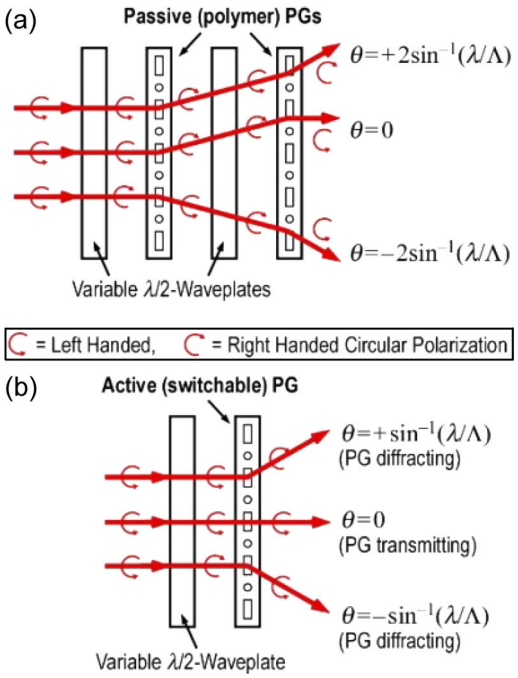

Fig. 17. ***Primary configurations of a single LCPG wide-angle steering stage using (a) two passive PGs and (b) one active PG.***

completely continuous wide-angle steering system can be implemented by adding a single fine-angle steering module (e.g., a liquid crystal spatial light modulator). As illustrated in Fig. 18, each PG stage incrementally contributes to the deflection angle as it is turned on, but always adds to the loss. Therefore, the number of stages within the beam-steering stack limits the overall efficiency, which is strongly affected by four factors—steering efficiency, scatter, absorption, and Fresnel loss—which could be significant.

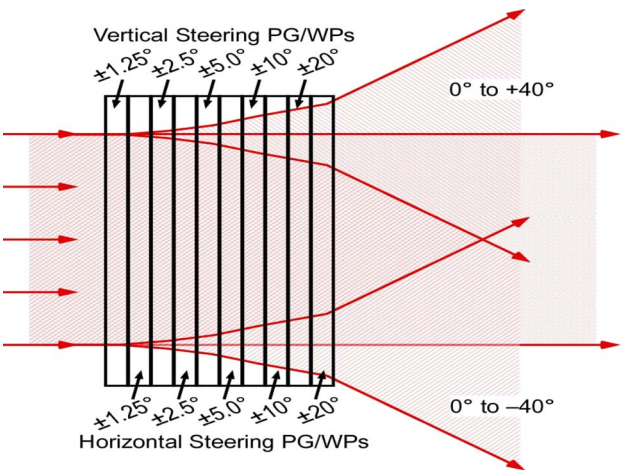

Fig. 18. ***Detail of the coarse, binary (PG) module.***

For example, a 1550-nm system is being developed that will cover an 80° × 80° field of regard in 1.25° steps with a random-access rate of < 10 ms. To do this, five azimuth and five elevation steering stages (i.e., 1.25°, 2.5°, 5.0°, 10.0°, and 20.0°) are needed within a conventional digital steering stack. The ten stages represent ten polarization gratings and ten liquid crystal switches. If moderately best-in-class values are used for the different loss parameters, the cumulative loss estimates for the active and passive coarse steering devices are estimated as follows.

- *Steering loss* (fraction of received light not steered into the intended order): Current loss is < 1% per grating: 10 stages @ 1% per = 10% loss.
- *Fresnel loss* (due to index differences): Using optimal glass substrates and index-matching coatings, estimate 20 components @ 0.1% per = 1 − 0.99920 = 2% loss.
- *Absorption* (due to the transparent conductor layers): Estimate < 1% at 1550 nm each layer, with 40 layers @ 1% = 1 − 0.99340 = 24% loss, if standard Indium Tin Oxide (ITO) is used. An alternate transparent conductor can make a major difference, as discussed below.
- *Scatter* (light randomly scattered by the PGs): Need current best in class to stay below 0.5% loss. Current loss is < 0.3% for the best passive gratings. 10 stages @ 0.5% per = 5% loss.

From this loss analysis, the 80° × 80° stepper with 1.25° resolution will have an overall efficiency of approximately 60%, with most of the loss coming from transparent conductor absorption (in this case ITO). If the system is instead built using 1000-Ω/sq Transcon, transparent conductors developed by Teledyne Scientific, which are expected to have < 0.1% absorption at 1500 nm, then system throughput increases to ~80%. Novel configurations of the PGs and waveplates are being studied that can reduce the number of components needed in the stack and could reduce losses [19]. Using novel schemes up to 87% efficiency over an 80° × 80° steering field of view is shown as possible, with 1.25° steering increments. Further improvement requires PGs with even more ideal properties, which should be possible as the fabrication techniques mature and device development moves from visible to near-IR, where there is more tolerance to slight fabrication errors. With careful engineering, this approach, combined with narrow field of regard LC steering, should be able to achieve > 90% efficiency over a very wide field of view.

This approach has the potential to be inexpensive to manufacture.

IV. ALTERNATE NONMECHANICAL STEERING APPROACHES

A. Lenslet Array-Based Steering

In this section, we explore a microlens array implementation of fixed period, variable blaze (or order) beam

steering that makes use of three cascaded arrays [28], [71]. There are two reasons to investigate lenslet-based beam steering. One is because there are no physical resets, only a jump in the first derivative of phase. This can eliminate the flyback region associated with sawtooth phase profiles, thus increasing maximum steering efficiency. The second reason is, for large lenslet beam steering, we will need almost four times less OPD in a given layer then using an LC sawtooth profile. The main disadvantage of lenslet-based beam steering is it has multiple layers. Each layer adds complexity and can reduce steering efficiency due to mundane engineering factors such as absorption, reflection, and scattering.

A single triplet of the cascaded arrays is shown in Fig. 19.

Early work only used a doublet for steering [72], [73]. The reason for going to three lenses in later work is because a field lens between the two lenslets redirects light such that essentially all of the light passing through the first lens will reach the last lens [27]. From Fig. 19, it can be seen that the steering angle is given by

$$\tan\theta = \frac{\Delta x}{f} \tag{13}$$

where Δx is the amount of decenter of the first microlens with respect to the optical axis of the other two microlenses and f is the common focal length of all three microlenses in the triplet. Steering is based on changing the diffractive orders, so a phase corrector plate needs to be used to dither the angular location of orders [74], or a fine angle beam steerer must be used to steer between orders [72]. An example of steering to discrete angles is shown in Table 3.

At F1, we can achieve steering up to 25°, so this can be a moderately wide-angle steering approach, as well as moving to high efficiency. Creating the moving microlens array electronically allows very precise positioning of the array since the positioning is based upon electrode spacing and applied voltages.

Table 3 Lenslet Steering Parameters

Δx, μm	Steering angle, degrees	Focal Length, μm	Lenslet Diameter μm	F#	OPD, μm
67.5	25	145	150	1	19.4
67.5	20	185	150	1.2	15.2
67.5	10	383	150	2.6	7.3
67.5	3	1288	150	8.6	2.2
67.5	1.5	2578	150	17.2	1.1

For simplicity, we assume microlens elements are plano-convex, as illustrated in Fig. 20.

We can calculate d, which is the required OPD to make the lens of a given thickness, using the standard sag formula

$$\text{OPD} = (n-1)d = \frac{\rho^2}{2f} \tag{14}$$

where n is the index of the microlens. From (5), we can see that if Δx $= \rho$, the radius of the microlens, that the lenslet array will steer to the maximum allowed angle. Using (13) with Δx $= \rho$ and (14), we can see that

$$\text{OPD} = \frac{\rho}{2}\tan(\theta_{\max}). \tag{15}$$

The effective resets would be at the spacing of the lenslet arrays. For small angles, we can make sine and tangent equivalent. The result is that we need an OPD four times thinner than a triangular profile phase to have the ability to steer to the maximum angle in a lenslet array. Of course we cannot steer out to the full radius of the lenslets and have good beam quality. A factor of 3.5 reduction in OPD using this approach is a good estimate.

The best method of doing fine-angle beam steering is by adding up to a one-wavelength phase delay behind each lenslet in one of the lenslet arrays [14], [74]. This additional phase delay dithers the location of the orders of the fixed period beam steerer. The additional phase

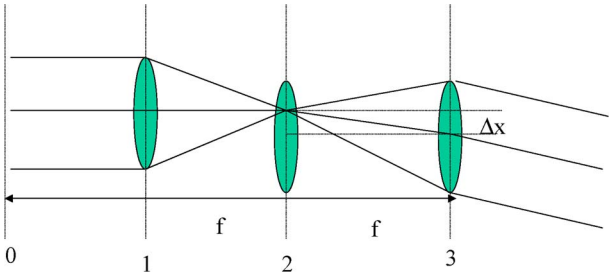

Fig. 19. *Lenslet array beam steering.*

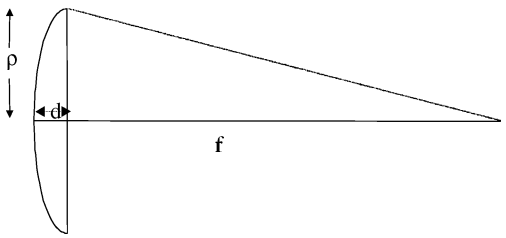

Fig. 20. *All positive lenslet microlens geometry.*

delay can be included in one of the lenslet arrays or can be a separate, fourth layer, depending on which is easier to implement.

An alternate lenslet-based steering approach can use a mixed set of lenslet arrays, with both positive and negative lenslets. This approach is shown in Fig. 20. The mixed lenslet approach eliminates the foci, thus increasing power handling capability [75]. The second major advantage of a mixed lenslet approach for beam steering is that lenslets are not required to have the ability to focus. An issue that occurs with the all-positive lenslet arrays is that there exists a minimum required OPD or each lenslet is not of high quality. If lenslets become too small and have a high F#, then the "focus" is in the far field of the lenslet. This means the lens does not have a quality focus. For mixed lenslet, the focused beam only is half the distance to a focus before it is diverged again by the negative lenslet. In that case, a focus is not required.

Fig. 21 shows a lenslet steering approach without an internal focus. This approach is previously discussed for a single set of lenses. [75]. The focal length of the positive lenslets is twice the focal length of the al-positive lenslet approach if the steering angle is kept constant. The negative lenslet requires a focal length half as large, but it could be implemented using a high index fixed material. This approach requires the two positive, outside, lenslet arrays to have identical focal lengths and to be placed one focal length apart. This is half the separation of the all-positive lenslet array approach.

For mixed lenslet steering, the center lenslet is moved down one unit while the positive lenslet on the other side is moved up two units. For a mixed lens approach

$$\theta = \arctan\left(\frac{2\Delta x}{f}\right). \tag{16}$$

In (16), f is the focal length of the positive lenslets. The focal length of the negative lenslet is one-fourth that of the positive lenslet. Digital simulations showed the mixed lenslet approach having $> 98\%$ steering efficiency for small angles such as 1.5°. The middle lenslet could, however, still clip energy entering the first lenslet. The main issue on efficiency will, however, be loss through multiple layers.

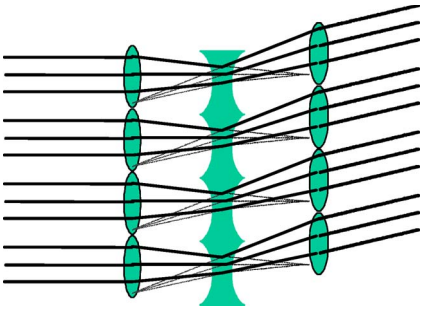

Fig. 21. *Lenslet array steering configuration without an internal focus.*

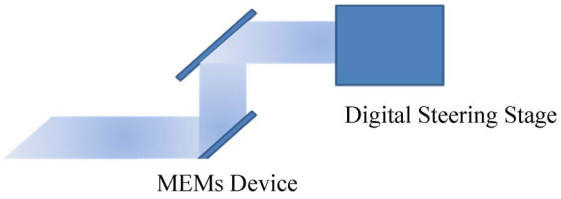

Fig. 22. *Reflective geometry for fine-angle steering.*

B. MEMS-Based Laser Beam Steering

MEMS mirrors are another steering option [76]. Individual mirrors are dispersion-free and polarization-invariant. Large single-aperture mirrors are bulky and slow, however, and they consume high power. Using the same optical phased array concept, a large single-aperture mirror can be divided into an array of much smaller aperture MEMS mirrors. The MEMS mirrors are much faster because they have much lower mass and inertia. But in order to form a phased array, we need to provide a 2π phase shift between the MEMS mirrors. A 2π phase shift can be provided either by moving each mirror vertically or by adding a phase shift layer before each micromirror. The phase layer only has to be a π phase layer to provide 0 to 2π phase shift since we are in a reflective mode. At the same time, the micromirrors must generate angular rotation to steer the light beam.

MEMS mirror-based steering has to operate in a reflective mode. The need to make the steering elements reflective can increase the size of a steering system. At the same time, MEMS mirrors could be used to steer prior to a digital stage, such as shown in Fig. 22. With a MEMS mirror beam steerer, both azimuth and elevation can be steered on one surface rather than separating azimuth and elevation steering, such as occurs with reflective liquid crystal arrays.

There is no flyback region with MEMS mirrors. Due to size of the MEMS mirrors, the best method of steering is by tilting the micromirrors. Since this is not a piston steering approach, there is no digitization loss. This removes the two major loss mechanisms associated with sawtooth-based LCs. If either a piston motion can be used for phasing between phase ramps or a separate phase layer, then this can be a very high-efficiency steering method. Fill factor will need to be addressed to keep high throughput efficiency with MEMS steering. Combination of a reflective array of MEMS mirrors with a step-steering approach could be very efficient over wide angles.

Texas Instruments (TI) pioneered development of MEMS mirror arrays for displays [77], while Lucent was

the lead to apply MEMS mirror array for optical communications [78]. However, these TI or Lucent MEMS mirrors do not have phase, or piston control. On the other hand, Stewart *et al.* demonstrated deformable micromirror arrays with piston actuation using a deformable membrane [79]. This type of micromirror arrays is mainly used for wavefront correction applications. Tuantranont *et al.* reported a phase-only micromirror array using flip-chip bonding and electrothermal actuation [80]. Lucent also reported a micromirror array design that can generate tip/tilt and piston (TTP) motions by using hidden lateral comb drives [81], [82], but the angular and piston ranges of the TTP mirrors are relatively small and compromise each other. All these efforts, however, are based on thin-film structures. The sizes of the mirrors with phase control are all about 100 μm. This kind of mirror size is too large for a stair-step phase profile. At the same time, a large number of micromirrors are needed to form a large effective aperture size of an OPA, which will result in a high complexity of the control electronics. Also the radii of curvature of those thin-film mirrors are typically not high.

TTP micromirrors have been realized by various actuation mechanisms, including electrostatic vertical comb drives [83]–[87] and electrothermal bimorph actuators [88], [89]. Electrostatic actuation is fast and consumes low power but requires high drive voltages and has small linear and angular scan ranges. In contrast, electrothermal actuation achieves large linear and angular scan ranges at low voltages but has relatively slower speeds and consumes higher power. Milanovic *et al.* 2004 demonstrated an electrostatic micromirror that has a mirror size of 0.6 mm and a response time of 0.2 ms [84]. Wu *et al.* demonstrated an electrothermal micromirror that has a mirror size of >1.0 mm and a response time of about 3 ms, as shown in Fig. 23 [90]. Fabrication and characterization of a 4×4 micromirror array consisting of TTP electrothermal MEMS mirrors has also been reported [91]. Each micromirror has an optical aperture size of 0.5×0.5 mm^2. Both tip and tilt angles of over $\pm 30^\circ$ are obtained with less than 5 V_{dc}. The piston displacement reaches 215 μm at 4 V_{dc}. Two-dimensional scanning was demonstrated. The thermal response time of the micromirrors is about 10 ms.

For MEMS mirror arrays, it is critical to have high-area fill factors. One way to boost fill factors is to use hidden actuators, i.e., microactuators are placed under mirror plates. Hidden actuators can be easily implemented in thin-film surface-micromachining processes [92], [93]. One example is TI's digital micromirror devices, which have small pixel sizes. The fabrication of single-crystal silicon (SCS)-based hidden actuators for large-subaperture TTP micromirror arrays is much more challenging. The commonly used approaches are to transfer single-crystal silicon mirrors via capillary fluidic self-assembling [94], manual assembling [84], photoresist wafer gluing [85], or wafer-to-wafer bonding plus flip-chip bonding [86], [95], [96]. Wafer-level bonding requires several wafer bonding steps, resulting in high cost and low yield. Manual transfer does not provide high accuracy and reproducibility. Flip-chip bonding is a good compromise. To date, only small SCS TTP micromirror arrays (less than 6×6) have been demonstrated.

MEMS micromirror-based OPAs have the advantages of low insertion loss and no change of polarization. The only dispersion comes if a phase mismatch occurs at the reset. High-area fill factors can be obtained by utilizing hidden actuators. Large arrays of thin-film TTP micromirrors have been demonstrated but suffer from the limitations of mirror flatness, mirror size, scan range, and complexity of control electronics. SCS-based TTP micromirror arrays also have been reported to achieve large subaperture sizes, high mirror flatness, large scan range, and simple control electronics, but the fabrication processes are generally more complex, and the large arrays of such SCS micromirror-based OPAs have not been realized. MEMS mirror arrays need to have very high reflectivity in order to handle high powers, since the thermal path for cooling is very slow.

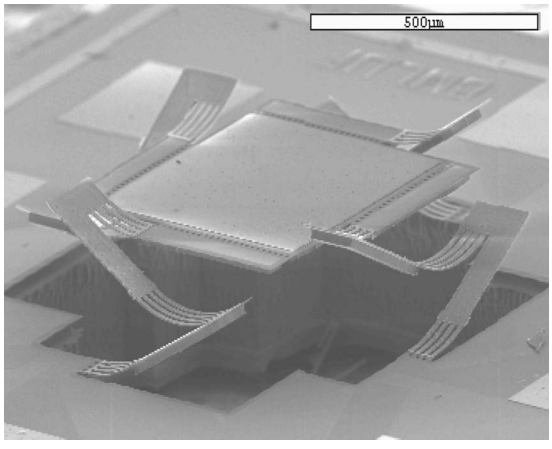

Fig. 23. *A tip/tilt/piston micromirror.*

C. Electrowetting-Based Beam Steering

Electrowetting has recently become another interesting option for steering optical beams. Initially people thought in terms of making lenslets by moving bubbles of liquid around. This is an interesting option that would be similar to lenslet-based steering, but it would be very difficult to prevent adjacent bubbles from coalescing. As an alternative, the University of Cincinnati has led the way toward using small boxes that contain low index water and high index oil. As shown in Fig. 24, the sidewalls of the boxes each have an electrode that modulates the liquid surface-wetting contact angle.

A prism geometry is created by applying sufficient voltage to any two opposing sidewalls to create a straight

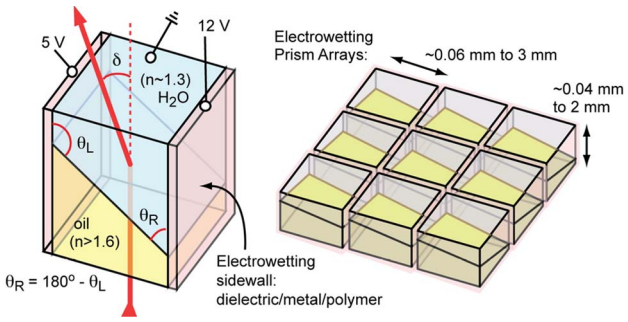

Fig. 24. ***Diagrams of basic operation of an electrowetting prism, with rough dimensions.***

but tilted interface between the water and oil [97]. Electrowetting can easily change the apex angles of the prism by a much as $+/-45°$. This could allow transmissive beam steering out to $+/-45°$. Of course, this approach could be combined with one of the large-angle step-steering approaches discussed earlier. Compression and transmission ratios [7] for the device can reduce the net beam-steering efficiency to ~50% at the maximum steering angles, but this limitation is not unique to this approach.

This electrowetting approach is a fixed-period beam-steering approach. Steering in an array of titled surfaces will occur by changing the order of the blaze. If an additional phase layer is utilized, then continuous steering can be achieved. The additional layer could be a liquid crystal layer. The size of these elements can be up to a few millimeters. This makes it an interesting candidate for broadband beam steering with larger resets. Electrowetting can be used in either reflective or transmissive modes. Electrowetting can steer to large angles in a transmissive mode, and a liquid crystal layer can provide phase matching between tilted segments, for the design wavelength. For a wavelength other then the design wavelength, we will still have moderate angular resolution because titled segments as large a 3 mm can be manufactured.

There are other factors for electrowetting prisms that should be briefly discussed. Switching speed should be on the order of 1 ms for the smallest prisms (tens of micrometers) and tens to hundreds of milliseconds for millimeter-sized prisms [98]. This size dependence is because electrowetting is an electromechanical effect requiring movement of mass (i.e., the liquids). Optical absorption is practically a nonissue in the visible and NIR. However, for wavelengths $> 2\ \mu$m, it is well understood that the water inside the prism will be a strong absorber. To remedy this, either the water must be replaced with a different liquid or the prisms must be very small (tens of micrometers high) to minimize optical absorption. Electrowetting can also provide reflective mode operation, as demonstrated recently by suspending a multilayer dielectric reflector film between the water/oil interface [99]. So long as the optical power is incident on the oil side of the device, operation well out into the infrared is possible with the right choice of dielectric mirror and oil materials. Because the reflection from the mirror occurs inside a high refractive index oil ($n > 1.6$), the additional refraction of the beam as it exits the device easily allows course steering over all angles contained within an entire hemisphere. However, like MEMS and lenslets, an additional phasing layer is required. Lastly, it should be noted that electrowetting prism arrays now in development utilize fabrication tools like those found in a liquid crystal display fabrication facility. Therefore electrowetting prism arrays might be scalable to larger apertures, possibly even > 10 cm, and fabrication should not be expensive.

D. Vertical Continuous Optical Phased Arrays

As discussed above, LC optical phased arrays usually follow the idea of generating a linear change of OPD across the aperture, while using resets to keep the required OPD small. Resets then impose a flyback region, reducing efficiency. As an alternative, the V-COPA devices discussed here use the same basic physics as the QHQ device of Pancharatam, discussed earlier. The difference is the steering angle of a single V-COPA device is variable instead of fixed like the previously discussed polarization gratings. V-COPA devices also have approximately 99.5% diffractive steering efficiency, similar to birefringent prisms [100].

The LCPGs discussed earlier achieve their spiral structure through the use of an alignment layer that has the desired spiral structure. This approach obviously does not yield a tunable device. Kent State has demonstrated a variable device called the V-COPA [100].

The basic structure of the device is shown in Fig. 25 by Shi of Kent State. The alignment is approximately vertical at the top and bottom substrates. The alignment is quasi-vertical alignment because in some domains the alignment is not exactly vertical but slightly tilts to the left, right, or in and out of the plane of the paper. For example, the alignment over electrode #1 and #2, and over the gap between them, is slightly pointed into the plane of the

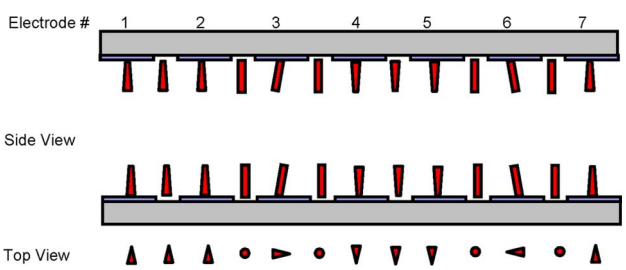

Fig. 25. ***V-COPA alignment setup.***

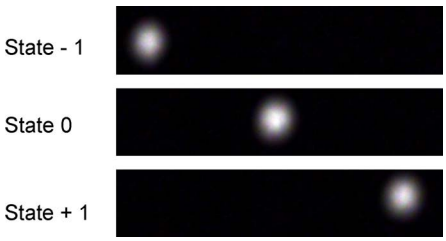

Fig. 26. *Deflected beams using the Kent State V-COPA device.*

paper. Similarly, the alignment over electrode #3 is slightly pointed to the right, while the alignment over electrode #6 is pointed to left. All the other region's alignment keeps the initial vertical direction.

The cell is filled with $-\Delta\varepsilon$ LC materials, so when a voltage is applied to cause an E-field that is vertical in the figure, the LC directors will distribute in the *x-y* plane. The helical sense adopted is controlled by the slight tilting of the director alignment layer.

The tipping of the director to the left and right in Fig. 25 can be controlled by fringing fields resulting from the voltage pattern applied to the in-plane cell electrodes. In this way, the regions tilting to the left or right can be controlled and the sense of the helix can be electrically controlled.

Fig. 26, taken by Shi at Kent State, shows the steering of a 1.5 μm laser beam passing through a test device. State 0 corresponds to the case when no voltage is applied to the device, and so no helix is present, and the beam is not defected. The +1 states are with voltage applied to cause the formation of a spiral structure. The fringing fields from the electrodes have been used to cause these two states to have a different helical sense and therefore to cause the laser beam to be steered in different directions.

By controlling the voltages applied to the electrodes, the period of the helix can be changed. Tunable steering angle can be achieved. The main focus of current work on V-COPA is switching speed. If speed is sufficient, then this will become a very attractive steering approach. It has high diffractive efficiency, like the birefringent prisms, but will require fewer layers. It is not clear that tunable devices will be manufacturable to steer to as large and angle as the fixed devices, so a future combination of VCOPA with a large angle step-steering approach like birefringent prisms is likely.

V. SUMMARY

Many interesting design options are becoming available for nonmechanical steering of narrow linewidth radiation. The significant efficiency limitations of traditional sawtooth phase profile LC-based steering are being overcome by a combination of attractive step-steering approaches and alternate continuous steering approaches. Fixed angle, step steering, polarization gratings provide a very high-efficiency alternative method of large-angle step steering. Due to a large acceptance angle, they will allow steering of images. Because each additional grating doubles or triples the number of steering states, they allow use of a single small-angle continuous steering element while steering to very large angles such as plus or minus 40°. This reduces the effect of the inefficiency of the sawtooth liquid crystal steering approach. Variable birefringent gratings, V-COPA, have recently been developed that provide breakthrough diffractive efficiency levels in a continuous steering approach. If speed is sufficient, this approach probably will replace conventional sawtooth liquid crystal steering. Lenslet-based steering, or MEMS, are other possible replacements for the continuous steering element, usually employing sawtooth phase profile liquid crystals. Lenslet steering can also provide a very efficient method of continuous steering when combined with a 0 to 2π phase layer. The major challenge with lenslet steering is the number of device layers required. Electrowetting can provide high-efficiency continuous steering in both dimensions, to large angles, using a single two-dimensional steering layer plus a 0 to 2π phase layer. Holographic gratings are very efficient for large-angle step steering. In the future, they could be combined with more efficient continuous steering approaches. The major limitations of volume holographic gratings are the requirement for continuous steering before and after and the fact that doubling the number of steering states requires twice as many elements. More efficient continuous steering approaches mitigate these effects. We are coming much closer to performance options that will allow nonmechanical beam steering to a faction of the diffraction limit over very wide angles. These devices are finally capable enough so electrooptical system designers will begin to adopt them. The availability of large angle, high efficiency, nonmechanical steering options will significantly improve future electro-optics systems. ■

REFERENCES

[1] T. A. Dorschner and D. P. Resler, "Optical beam steerer having subaperture addressing," U.S. Patent 5 093 740, Mar. 3, 1992.

[2] P. F. McManamon, E. A. Watson, T. A. Dorschner, and L. J. Barnes, "Nonmechancial beam steering for active and passive sensors," in *Proc. SPIE 1417*, 1991, vol. 110, p. 194.

[3] P. F. McManamon, J. Shi, and P. Bos, "Broadband optical phased-array beam steering," *Opt. Eng.*, vol. 44, p. 128 004, 2005.

[4] J. Goodman, *Introduction to Fourier Optics*. San Francisco, CA: McGraw-Hill, 1968, p. 65.

[5] J. Frank and J. D. Richards, "Phased array radar antennas," in *Radar Handbook, Merrill Skolnik*, 3rd ed. New York: McGraw-Hill, pp. 13.2–13.3.

[6] E. A. Watson and L. J. Barnes, "Optical design considerations for agile beam steering," in *Proc. SPIE*, 1994, vol. 2120, pp. 186–193.

[7] J. Shi, P. J. Bos, B. Winker, and P. McManamon, "Switchable optical phased prism arrays for beam steering," in *Proc. SPIE*, 2004, vol. 5553, pp. 102–111.

[8] R. A. Meyer, "Optical beam steering using a multichannel lithium tantalite crystal," *Appl. Opt.*, vol. 11, pp. 613–616, Mar. 1972.

[9] Y. Nimomiya, "Ultrahigh resolving electrooptical prism array light deflectors," *IEEE J. Quantum Electron.*, vol. 9, pp. 791–795, Aug. 1973.

[10] F. Vasey, F. K. Reinhart, R. Houdre, and J. M. Staufer, "Spatial optical beam steering with AlGaAs integrated phased array," *Appl. Opt.*, vol. 32, pp. 3220–3232, June 1993.

[11] A. Tanone, Z. Zhang, C. M. Uang, and F. T. S. Yu, "Optical beam steering using a liquid-crystal television panel," *Microw. Opt. Technol. Lett.*, vol. 7, pp. 285–289, Apr 1994.

[12] A. F. Fray and D. Jones, "Liquid crystal light deflector," U.S. Patent 4 066 334, 1978.

[13] R. M. Matic, "Blazed phased liquid crystal beam steering," *Proc. Soc. Photo Opt. Instrum. Eng. Laser Beam Propag. Contr.*, vol. 2120, pp. 194–205, 1994.

[14] P. F. McManamon, T. A. Dorschner, D. C. Corkum, L. J. Friedman, D. S. Hobbs, M. K. O. Holz, S. Liberman, H. Nguyen, D. P. Resler, R. C. Sharp, and E. A. Watson, "Optical phased array technology," *Proc. IEEE*, vol. 84, no. 2, pp. 268–298, 1996.

[15] R. C. Sharp, D. P. Resler, D. S. Hobbs, and T. A. Dorschner, "Electrically tunable liquid-crystal wave plate in the infrared," *Opt. Lett.*, vol. 15, no. 1, pp. 87–89, 1990.

[16] D. P. Resler, D. S. Hobbs, R. C. Sharp, L. J. Friedman, and T. A. Dorschner, "High-efficiency liquid-crystal optical phased-array beam steering," *Opt. Lett.*, vol. 21, no. 9, pp. 689–691, 1996.

[17] J. P. Huignard, A. M. Roy, and C. Slezak, "Electro-optical deflection apparatus using holographic grating," U.S. Patent 3 980 389, Sep. 14, 1976.

[18] I. W. Smith and M. K. O. Holz Wide angle beam steering system, U.S. Patent 7 215 472, May 8, 2007.

[19] N. A. Riza, "BOPSCAN technology, a methodology and implementation of the billion point optical scanner," in *Proc. SPIE*, Sep. 1998, vol. 3482, pp. 572–578.

[20] J. Kim, C. Oh, M. J. Escuti, L. Hosting, and S. Serati, "Wide-angle nonmechanical beam steering using thin liquid crystal polarization gratings," in *Proc. SPIE Adv. Wavefront Contr.: Methods, Devices, Applicat. VI*, 2008, vol. 7093.

[21] P. F. Van Kessel, L. J. Hornbeck, R. E. Meier, and M. R. Douglass, "A MEMS-based projection display," *Proc. IEEE*, vol. 86, pp. 1687–1704, Aug. 1998.

[22] R. S. Muller and K. Y. Lau, "Surface-micromachined microoptical elements and systems," *Proc. IEEE*, vol. 86, pp. 1705–1720, Aug. 1998.

[23] R. T. Howe, R. S. Muller, K. J. Gabriel, and W. S. N. Trimmer, "Silicon micromechanics: Sensors and actuators on a chip," *IEEE Spectrum*, vol. 27, pp. 29–31, Jul. 1990.

[24] H. Fujita, "Microactuators and micromachines," *Proc. IEEE*, vol. 86, pp. 1721–1732, Aug. 1998.

[25] Krishnamoorthy, K. Li, K. Yu, D. Lee, J. P. Heritage, and O. Solgaard, "Dual mode micromirrors for optical phased array applications," *Sens. Actuators A, Phys.*, vol. A97–98, pp. 21–26, Apr. 2002.

[26] E. A. Watson and A. R. Miller, "Analysis of optical beam steering using phased micromirror arrays," in *Proc. SPIE*, 1996, vol. 2687, pp. 60–67.

[27] N. R. Smith, D. C. Abeysinghe, J. W. Haus, and J. Heikenfeld, "Agile wide-angle beam steering with electrowetting microprisms," *Opt. Express*, vol. 14, pp. 6557–6563, 2006.

[28] E. A. Watson, "Analysis of beam steering with decentered microlens arrays," *Opt. Eng.*, vol. 32, no. 11, pp. 2665–2670, 1993.

[29] L. Shi, P. F. McManamon, and P. J. Bos, "Tunable liquid crystal optical phase plate with a large continuous in-plane gradient," *J. Appl. Phys.*, Aug. 7, 2008.

[30] Y.-H. Lin *et al.*, "Compact 4 cm aperture transmissive liquid crystal phased array for free space optical communications," in *Proc. SPIE*, 2005, vol. 5892.

[31] M. Mahajan, B. Wen, V. Bhupathy, D. Taber, and B. Winker, "Voltage calibration of dual frequency liquid crystal devices for infrared beam steering applications," in *Proc. SPIE*, vol. 5892.

[32] J. L. West, K. Zhang, M. Zhang, E. Buyuktanir, and A. Glushchenko, "Stressed liquid crystals and their application," in *Proc. SPIE Liquid Crystals IX*, I.-C. Khoo, Ed., Aug. 20, 2005, vol. 5936.

[33] H. Ren and S. T. Wu, "A liquid crystal-based linear polarization rotator with gradient refractive index," *Appl. Phys. Lett.*, vol. 81, p. 3537, 2002.

[34] Y. H. Wu, Y. H. Lin, Y. Q. Lu, H. Ren, Y. H. Fan, J. R. Wu, and S. T. Wu, "Submillisecond response variable optical attenuator based on sheared polymer network liquid crystal," *Opt. Express*, vol. 12, no. 25, pp. 6377–6384, Dec. 13, 2004.

[35] B. Wang, G. Zhang, A. Glushchenko, J. L. West, P. J. Bos, and P. F. McManamon, "Stressed liquid- cyrstial optical phased array for fast tip-tilt wavefront correction," *Appl. Opt.*, vol. 44, no. 36, Dec. 20, 2005.

[36] D. A. Coleman, J. Fernsler, N. Chattham, M. Nakata, Y. Takanishi, E. Korblova, D. R. Link, R. F. Shao, W. G. Jang, J. E. Maclennan, O. Mondainn-Monval, C. Boyer, W. Weissflog, G. Pelzl, L. C. Chien, J. Zasadzinski, J. Watanabe, D. M. Walba, H. Takezoe, and N. A. Clark, "Polarization-modulated smectic liquid crystal phases," *Science*, vol. 301, pp. 1204–1211, 2003.

[37] P. F. McManamon, "Agile nonmechanical beam steering," *Opt. Photon. News*, pp. 21–25, Mar. 2006.

[38] X. Wang, B. Wang, P. F. McManamon, J. J. Pouch, F. A. Miranda, J. E. Anderson, and P. J. Bos, "Spatial resolution limitation of liquid crystal spatial light modulator," in *Proc. Liquid Cryst. Conf. Great Lakes Photonics Symp.*, Cleveland, OH, Jun. 7–11, 2004.

[39] S. Harris, "Characterization and application of a liquid crystal beam steering device," in *Proc. SPIE*, 2001, vol. 4291, pp. 109–119.

[40] S. Harris, "Polarization effects in nematic liquid crystal optical phased arrays," *Proc. IEEE*, vol. 5213, pp. 26–39, 2004.

[41] H. Kogelnik, "Coupled wave theory for thick hologram gratings," *Bell Syst. Tech. J.*, vol. 48, no. 9, pp. 2909–2947, Nov. 1969.

[42] I. V. Ciapurin, L. B. Glebov, and V. I. Smirnov, "Modeling of Gaussian beam diffraction on volume Bragg gratings in PTR glass," in *Proc. SPIE Practical Hologr. XIX: Mater. Applicat.*, Bellingham, WA, 2005, vol. 5742.

[43] N. A. Riza and M. A. Arain, "Code-multiplexed optical scanner," *Appl. Opt.*, vol. 42, no. 8, pp. 1493–1502, Mar. 2003.

[44] Z. Yaqoob, M. A. Arain, and N. A. Riza, "High-speed two-dimensional laser scanner based on Bragg gratings stored in photothermorefractive glass," *Appl. Opt.*, vol. 42, no. 26, pp. 5251–5262, Sep. 10, 2003.

[45] Z. Yaqoob and N. A. Riza, "Free-space wavelength-multiplexed optical scanner demonstration," *Appl. Opt.*, vol. 41, no. 26, pp. 5568–5573, Sep. 10, 2002.

[46] L. Glebov, "Fluorinated silicate glass for conventional and holographic optical elements," in *Proc. SPIE Window Dome Technol. Mater. X*, 2007, vol. 6545, p. 654 507.

[47] N. Vorobiev, L. Glebov, and V. Smirnov, "Single-frequency-mode Q-switched Nd: YAG and Er:Glass lasers controlled by volume Bragg gratings," *Opt. Express*, vol. 16, no. 12.

[48] L. Glebov, "Volume Bragg gratings in PTR glass—New optical elements for laser design," presented at the 23rd Advanced Solid-State Photonics (ASSP) Topical Meeting, Nara, Japan, paper code MD1, unpublished.

[49] Raytheon steered agile beams, STAB, Final Rep. AFRL-SN-WP-TR-2004-1078.

[50] U. Schmidt and W. Hust, "Optical deflection system including an alternating sequence of birefringent prisms and polarizers," U.S. Patent 3 572 895, Dec. 1986.

[51] H. Meyer, D. Riekmann, K. P. Schmidt, U. J. Schmidt, M. Rahlff, E. Schrbder, and W. Thust, "Design and performance of a 20-stage digital light beam deflector," *Appl. Opt.*, vol. 11, no. 8, pp. 1932–1736, Aug. 1972.

[52] M. A. Karim, D. Cook, and P. F. McManamon, "Digital beam steering system using modules of ferro electric liquid crystal and Wollaston prism," in *Tech. Dig. 1988 Annu. Meeting Opt. Soc. Amer.*, Santa Clara, CA, Oct. 1988, p. 118.

[53] C. M. Titus, P. J. Bos, and O. D. Lavrentovich, "Efficient, accurate liquid crystal digital light deflector," in *Proc. SPIE*, 1999, vol. 3633, p. 244.

[54] S. A. Khan and N. A. Riza, "Demonstration of 3-dimensional wide angle laser beam scanner using liquid crystals," *Opt. Express*, vol. 12, no. 5, pp. 868–882, Mar. 8, 2004.

[55] V. R. L. Sutherland and L. V. Natarajan, "Development of photopolymer liquid crystal composite materials for dynamic hologram applications," in *Proc. SPIE Diffract. Holograph. Opt. Technol.*, I. Cindrich and S. H. Lee, Eds., 1994, vol. 2152, pp. 303–313.

[56] R. L. Sutherland, "Electrically switchable volume holographic gratings in polymer-dispersed liquid crystals," *Appl. Phys. Lett.*, vol. 64, pp. 1074–1076, 1994.

[57] L. H. Domash, T. Chen, B. N. Gomatam, C. M. Gozewski, R. L. Sutherland, L. V. Natarajan, V. P. Tondiglia, T. J. Bunning, and W. W. Adams, "Switchable-focus lens in holographic polymer-dispersed liquid crystal," in *Proc. SPIE Diffract. Holograph. Opt. Technol. III*, I. Cindrich and S. H. Lee, Eds., 1996, vol. 2689, pp. 188–194.

[58] S. Pancharatnam, "Achromatic combination of birefringent plates," in *Proc. Indian Acad. Sci.*, 1955, vol. XLI, no. 4, p. 137, sec. A.

[59] M. J. Escuti and W. M. Jones, "Polarization independent switching with high contrast from a liquid crystal polarization grating," in *SID Symp. Dig.*, 2006, vol. 37, pp. 1443–1446.

[60] M. J. Escuti and W. M. Jones, "A polarization-independent liquid crystal spatial-light-modulator," in *Proc. SPIE Opt. Photon. Conf.*, 2006, vol. 6332, p. 633 222.

[61] R. Komanduri, W. M. Jones, C. Oh, and M. J. Escuti, "Polarization-independent modulation for projection displays using small-period LC polarization gratings," *J. Soc. Inf. Display*, vol. 15, pp. 589–594, 2007.

[62] M. J. Escuti, C. Oh, C. Sanchez, C. Bastiaansen, and D. J. Broer, "Simplified spectropolarimetry using reactive mesogen polarization gratings," in *Proc. SPIE Opt. Photon. Conf.*, 2006, vol. 6302, p. 630 207.

[63] J. Eakin, Y. Xie, R. Pelcovits, M. D. Radcliffe, and G. P. Crawford, "Zero voltage Freedericksz transition in periodically aligned liquid crystals," *Appl. Phys. Lett.*, vol. 85, pp. 1671–1673, 2004.

[64] M. J. Escuti and W. M. Jones, "Polarization independent switching with high contrast from a liquid crystal polarization grating," in *SID Symp. Dig.*, 2006, vol. 37, pp. 1443–1446.

[65] M. J. Escuti and W. M. Jones, "A polarization-independent liquid crystal spatial-light-modulator," in *Proc. SPIE Opt. Photon. Conf.*, 2006, vol. 6332, p. 633 222.

[66] R. Komanduri, W. M. Jones, C. Oh, and M. J. Escuti, "Polarization-independent modulation for projection displays using small-period LC polarization gratings," *J. Soc. Inf. Display*, vol. 15, pp. 589–594, 2007.

[67] C. Provenzano, G. Cipparrone, and A. Mazzulla, "Photopolarimeter based on two gratings recorded in thin organic films," *Appl. Opt.*, vol. 45, pp. 3929–3934, 2006.

[68] R. Komanduri, W. M. Jones, C. Oh, and M. J. Escuti, "Polarization-independent modulation for projection displays using small-period LC polarization gratings," *J. Soc. Inf. Display*, vol. 15, pp. 589–594, 2007.

[69] C. Provenzano, G. Cipparrone, and A. Mazzulla, "Photopolarimeter based on two gratings recorded in thin organic films," *Appl. Opt.*, vol. 45, pp. 3929–3934, 2006.

[70] M. J. Escuti, C. Oh, W. M. Jones, C. Sanchez, C. Bastiaansen, and D. J. Broer, "Reactive mesogen polarization gratings with small pitch and ideal properties," Opt. Express, 2008, to be published.

[71] E. A. Watson, W. E. Whitaker, C. D. Brewer, and S. R. Harris, "Implementing optical phased array beam steering with cascaded microlens arrays," in *Proc. IEEE Aerosp. Conf.*, Mar 2002.

[72] W. Golsos and M. Holz, "Agile beam steering using binary optics microlens arrays," *Opt. Eng.*, vol. 11, no. 29, pp. 1392–1397, 1990.

[73] K. M. Flood, W. J. Cassarly, C. Sigg, and J. M. Finlan, "Continuous wide angle beam steering using translation of binary microlens arrays and a liquid crystal phased array," *Proc. SPIE Comput. Opt. Formed Holograph. Opt.*, vol. 1211, pp. 296–304, 1990.

[74] Y. H. Lin, M. Mahajan, D. Taber, B. Wen, and B. Winker, "Compact 4 cm aperture transmissive liquid crystal optical phased array for free-space optical communications," in *Proc. SPIE Free-Space Laser Commun.*, Aug. 31, 2005, vol. 5892, p. 58920C.

[75] J. L. Gibson, B. Duncan, E. A. Waston, and J. S. Loomis, "Wide-angle decentered lens beam steering for infrared countermeasures applications," *Opt. Eng.*, vol. 43, no. 10, pp. 2312–232, 2004.

[76] M. Kiang, O. Solgaard, K. Y. Lau, and R. S. Muller, "Electrostatic comb drive-actuated micromirrors for laser-beam scanning and positioning," *J. Microelectromech. Syst.*, vol. 7, no. 1, pp. 27–37, Mar. 1998.

[77] L. J. Hornbeck, "Digital light processing and MEMS: An overview," in *Proc. IEEE/LEOS 1996 Summer Topical Meetings*, Aug. 5–9, 1996, pp. 7–8.

[78] V. A. Aksyuk, S. Arney, N. R. Basavanhally, D. J. Bishop, C. A. Bolle, C. C. Chang, R. Frahm, A. Gasparyan, J. V. Gates, R. George, C. R. Giles, J. Kim, P. R. Kolodner, T. M. Lee, D. T. Neilson, C. Nijander, C. J. Nuzman, M. Paczkowski, A. R. Papazian, F. Pardo, D. A. Ramsey, R. Ryf, R. E. Scotti, H. Shea, and M. E. Simon, "238 × 238 micromechanical optical cross connect," *IEEE Photon. Technol. Lett.*, vol. 15, pp. 587–589, Apr. 2003.

[79] J. B. Stewart, T. G. Bifano, S. Cornelissen, P. Bierden, B. M. Levine, and T. Cook, "Design and development of a 331-segment tip-tilt-piston mirror array for space-based adaptive optics," *Sens. Actuators A, Phys.*, vol. 138, no. 1, pp. 230–238, 2007.

[80] A. Tuantranont, V. M. Bright, L.-A. Liew, W. Zhang, and Y. C. Lee, "Smart phase-only micromirror array fabricated by standard CMOS process," in *Proc. IEEE 13th Annu. Int. Conf. Micro Electro Mech. Syst. (MEMS 2000)*, 2000, pp. 455–460.

[81] R. Ryf, H. R. Stuart, and C. R. Giles, "MEMS tip/tilt & piston mirror arrays as diffractive optical elements," in *Proc. SPIE*, Bellingham, WA, 2005, vol. 5894, pp. 58940C-1–11.

[82] F. Pardo, M. E. Simon, V. A. Aksyuk, R. Ryf, W. Y. C. Lai, C. S. Pai, F. P. Klemens, J. F. Miner, R. A. Cirelli, E. J. Ferry, J. E. Bower, W. M. Mansfield, A. Kornblit, T. W. Sorsch, J. A. Taylor, M. R. Baker, R. Fullowan, H. Dyson, A. Gasparyan, Y. Low, D. Ramsey, and S. Arney, "Characterization of piston-tip-tilt mirror pixels for scalable SLM arrays," in *Proc. IEEE/LEOS Int. Conf. Optical MEMS Applicat. Conf.*, 2006, pp. 21–22.

[83] H. Xie, Y. Pan, and G. K. Fedder, "A CMOS-MEMS mirror with curled-hinge comb drives," *J. Microelectromech. Syst.*, vol. 12, no. 4, pp. 450–457, 2003.

[84] V. Milanovic, G. A. Matus, and D. T. McCormick, "Gimbal-less monolithic silicon actuators for tip-tilt-piston micromirror applications," *IEEE J. Sel. Topics Quantum Electron.*, vol. 10, no. 3, pp. 462–471, 2004.

[85] W. Piyawattanametha, P. R. Patterson, D. Hah, H. Toshiyoshi, and M. C. Wu, "Surface- and bulk- micromachined two-dimensional scanner driven by angular vertical comb actuators," *J. Microelectromech. Syst.*, vol. 14, no. 6, pp. 1329–1338, 2005.

[86] I. W. Jung, U. Krishnamoorthy, and O. Solgaard, "High fill-factor two-axis gimbaled tip-tilt-piston micromirror array actuated by self-aligned vertical electrostatic combdrives," *J. Microelectromech. Syst.*, vol. 15, no. 3, pp. 563–571, 2006.

[87] J. C. Tsai and M. C. Wu, "Design, fabrication, and characterization of a high fill-factor, large scan-angle, two-axis scanner array driven by a leverage mechanism," *J. Microelectromech. Syst.*, vol. 15, no. 5, pp. 1209–1213, 2006.

[88] A. Jain and H. Xie, "An electrothermal microlens scanner with low-voltage, large-vertical-displacement actuation," *IEEE Photon. Technol. Lett.*, vol. 17, no. 9, pp. 1971–1973, 2005.

[89] S. T. Todd, A. Jain, H. Qu, and H. Xie, "A multi-degree-of-freedom micromirror utilizing inverted-series-connected bimorph actuators," *J. Opt. A*, vol. 8, pp. 352–359, 2006.

[90] L. Wu and H. Xie, "A large vertical displacement electrothermal bimorph microactuator with very small lateral shift," *Sens. Actuators A*, vol. 145, pp. 371–379, 2008.

[91] L. Wu, S. Maley, T. Nelson, P. McManamon, and H. Xie, "A large-aperture, piston-tip-tilt micromirror for optical phase array applications," in *Proc. IEEE MEMS'08*, Tucson, AZ, 2008, pp. 754–757.

[92] L. J. Hornbeck, "Current status of the digital micromirror device (DMD) for projection television applications," in *Tech. Dig. Int. Electron Devices Meeting 1993.* Dec. 5–8, 1993, pp. 381–384.

[93] F. Pardo, R. A. Cirelli, E. J. Ferry, W. Y.-C. Lai, F. P. Klemens, J. F. Miner, C. S. Pai, J. E. Bower, W. M. Mansfield, A. Kornblit, T. W. Sorsch, J. A. Taylor, M. R. Baker, R. Fullowan, M. E. Simon, V. A. Aksyuk, R. Ryf, H. Dyson, and S. Arney, "Flexible fabrication of large pixel count piston-tip-tilt mirror arrays for fast spatial light modulators," *Microelectron. Eng.*, vol. 84, no. 5–8, pp. 1157–1161, 2007.

[94] U. Srinivasan, M. A. Helmbrecht, C. Rembe, R. S. Muller, and R. T. Howe, "Fluidic self-assembly of micromirrors onto microactuators using capillary forces," *IEEE J. Sel. Topics Quantum Electron.*, vol. 8, no. 1, pp. 4–11, 2002.

[95] S. Waldis, P. A. Clerc, F. Zamkotsian, M. Zickar, W. Noell, and N. de Rooij, "Micromirror arrays for object selection," in *Proc. SPIE*, San Jose, CA, Jan. 25–26, 2006, vol. 6114, pp. 611408.1–611408.12.

[96] P. J. Gilgunn and G. K. Fedder, "Flip-chip integrated SOI-CMOS-MEMS fabrication technology," in *Tech. Dig. Solid-State Sens., Actuators, Microsyst. Workshop*, Hilton Head Island, SC, 2008, pp. 10–13.

[97] N. R. Smith, D. C. Abeysinghe, J. W. Haus, and J. Heikenfeld, "Agile wide-angle beam steering with electrowetting microprisms," *Opt. Express*, vol. 14, pp. 6557–6563, 2006.

[98] N. R. Smith, L. Hou, J. Zhang, and J. Heikenfeld, "Experimental validation of >1 kHz electrowetting modulation," in *Proc. 17th Biennial University/Government/Industry Micro/Nano Symp. (UGIM 2008)*, Louisville, KY, Jul. 2008, pp. 11–14.

[99] L. Hou, N. R. Smith, and J. Heikenfeld, "Electrowetting manipulation of any optical film," *App. Phys. Lett.*, vol. 90, p. 251114, 2007.

[100] L. Shi, P. F. McManamon, and P. J. Bos, "Liquid crystal optical phase plate with a variable in-plane gradient," *J. Appl. Phys.*, vol. 104, p. 033109, 2008.

ABOUT THE AUTHORS

Paul F. McManamon (Fellow, IEEE) received the Ph.D. degree in physics from The Ohio State University, Columbus, in 1977.

He worked at Wright Patterson AFB from 1968 to 2008. His primary work with the Air Force Research Laboratory was in electrooptical sensors. He was Chief Scientist for the Avionics Directorate, Wright Lab, for more than two-and-a-half years. He was a Senior Scientist for infrared sensors for five years. He was Chief Scientist of the Sensors Directorate, Air Force Research Laboratory, from June 2005 to May 2008.

Dr. McManamon is a Fellow of SPIE, OSA, MSS, and the Air Force Research Laboratory. He was primary author of "Optical Phased Array Technology," which received the IEEE W. R. J. Baker award for the best paper in any IEEE referred journal or transaction. He was President of SPIE in 2006.

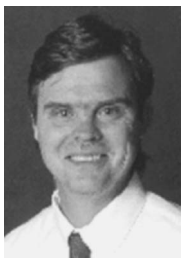

Philip J. Bos received the Ph.D. degree in physics from Kent State University, Kent, OH, in 1978.

After one year as a Research Fellow with the Liquid Crystal Institute, Kent State, he joined Tektronix Laboratories in the Display Research Department. In 1994, he returned to the Liquid Crystal Institute, where he is currently an Associate Director and a Professor of chemical physics. He currently has several projects in the area of applications of liquid crystals. He has more than 100 publications and has received 20 patents.

Michael J. Escuti (Member, IEEE) received the Ph.D. degree in electrical engineering from Brown University, Providence, RI, in 2002.

Since 2004, he has been an Assistant Professor of electrical and computer engineering at North Carolina State University at Raleigh, where he pursues interdisciplinary research topics in photonics, flat-panel displays, diffractive optics, remote sensing, and organic electronics. Prior to this, he spent two years with the functional-polymers group at Eindhoven University of Technology, The Netherlands, as a Postdoctoral Fellow. He has nine received or pending patents. He has published more than 60 refereed journal and conference publications and has presented 11 invited research talks.

Prof. Escuti received the Glenn H. Brown Award (2004) from the International Liquid Crystal Society and the OSA/New Focus Student Award (2002) from the Optical Society of America at the CLEO/QELS Conference for his Ph.D. research on electrooptical materials and their use in photonics and flat-panel displays.

Jason Heikenfeld (Senior Member, IEEE) received the B.S. and Ph.D. degrees from the University of Cincinnati, Cincinnati, OH, in 1998 and 2001, respectively.

During 2001–2005, he cofounded and was Principal Scientist with Extreme Photonix Corp. In 2005, he returned to the University of Cincinnati as an Assistant Professor in the Department of Electrical and Computer Engineering. His university laboratory, The Novel Devices Laboratory, is currently engaged in electrofluidic device research for beam steering, displays, and electronic paper. He has more than 80 publications and has presented nine invited talks. He has nine received or pending patents.

Dr. Heikenfeld is a member of SPIE and the Society for Information Display. He is an NSF CAREER and AFOSR Young Investigator. He is a member of the Board of Governors for the IEEE Lasers and Electro-Optics Society (LEOS) and an Associate Editor of the IEEE JOURNAL OF DISPLAY TECHNOLOGY. He was a past Technical Chair for Displays at the annual IEEE LEOS meeting.

Steve Serati received the B.S. and M.S. degrees in electrical engineering from Montana State University, Bozeman.

He is Founder and President of Boulder Nonlinear Systems, Inc. (BNS). Before starting BNS in 1988, he was a Design Engineer with Honeywell's Avionics Division for five years, Design Engineer and Project Manager with OPHIR Corporation for three years, and a System Engineer and Project Manager with Tycho Technology Inc. for two years. In addition to his duties as BNS' president, he is the Principal Investigator for developing nonmechanical beam-steering techniques for active and passive systems. He is responsible for improving BNS' spatial light modulator technologies that are being used for holographic optical trapping, pulse shaping, and wavefront correction.

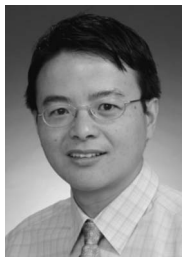

Huikai Xie (Senior Member, IEEE) received the M.S. degree in electrooptics from Tufts University, Medford, MA, in 1998 and the Ph.D. degree in electrical and computer engineering from Carnegie-Mellon University, Pittsburgh, PA, in 2002.

He is an Associate Professor in the Department of Electrical and Computer Engineering, University of Florida, Gainesville. From 1992 to 1996, he was a Faculty Member of the Institute of Microelectronics, Tsinghua University, Beijing. He has received four U.S. patents with 12 pending. He has published more than 100 technical papers. His present research interests include MEMS, NEMS, microsensors and microactuators, and photonics.

Prof. Xie was named a Researcher of the Year Finalist by *Small Times* in 2006.

Edward A. Watson received the B.S. degree in physics from the University of Arizona, Tempe. He received the M.S. degree in optical sciences and the Ph.D. degree in optics from the University of Rochester, Rochester, NY.

He is with the Electro-Optical Technology Division, Sensors Directorate, Air Force Research Laboratory, Wright-Patterson AFB, OH. He conducts research in active and passive electrooptic sensors, including the application of dynamic diffractive optical components to the agile steering and shaping of monochromatic and polychromatic light beams, development of multi-phenomenology laser radar imagers, and modeling of aliasing and blurring in sampled imagery.

Dr. Watson is a Fellow of SPIE, OSA, and the Air Force Research Laboratory.